Available online at www.sciencedirect.com
ScienceDirect
Tetrahedron
Tetrahedron 63 (2007) 12437–12445

New metallomesogens derived from unsymmetric 1,3,4-thiodiazoles: synthesis, single crystal structure, mesomorphism, and optical properties

Cheng-Tsung Liao,[a] Yueh-Ju Wang,[a] Chi-Shuen Huang,[a] Hwo-Shuenn Sheu,[b] Gene-Hsiang Lee[c] and Chung K. Lai[a,*]

[a]*Department of Chemistry, National Central University, and Center for Nano Science Technology, UST, Chung-Li 32054, Taiwan, ROC*
[b]*National Synchrotron Radiation Research Center, Hsinchu 30077, Taiwan, ROC*
[c]*Instrumentation Center, National Taiwan University, Taipei 10660, Taiwan, ROC*

Received 18 July 2007; revised 13 September 2007; accepted 13 September 2007
Available online 22 September 2007

Abstract—A series of copper(II) complexes **1** derived from unsymmetric 1,3,4-thiadiazoles **2** exhibiting mesogenic properties are reported. All the precursors **2** and **3** exhibited smectic A or/and smectic C phases, whereas, copper complexes formed nematic, SmA or SmC phases. The mesophases formed by derivatives **2** and **3** were probably attributed to the H-bondings induced both intramolecularly or/and intermolecularly between amide (–NH) and phenolic (–OH) groups. The crystal and molecular structures of mesogenic 2-(5-(2-(hexyloxy)naphthalene-6-yl)-1,3,4-oxadiazole-2-yl)phenol (**2**; n=6, m=6) were determined by means of X-ray structural analysis. It crystallizes in the monoclinic space group P-1, with a=7.4255(18) Å, b=8.209(2) Å, c=17.315(5) Å, and Z=2. An *intermolecular* H-bond (d=1.89 Å) between N2 and H1A atoms with an angle of 161.5° was observed. All molecules were packed as tilted layer arrangement and a π–π interaction (ca. 3.56 Å) was observed. Variable temperature FTIR and ^{1}H NMR spectroscopies were also used to probe the possible H-bondings formed in compound **2** (m=0, n=6). The fluorescent properties of these compounds **2** were examined. All λ_{max} peaks of the absorption and photoluminescence spectra occurred at ca. 359–363 nm and 519–537 nm, respectively. Excited state intramolecular proton transfer (ESIPT) reaction in this type of *ortho*-hydroxy-1,3,4-thiadiazole was also observed.

1. Introduction

1,3,4-Oxadiazole,[1] considered as an important five-membered compound among the huge heterocyclic families, has been studied as excellent candidate for material applications during the past years due to its excellent thermal, chemical stabilities and high photoluminescence quantum yields. These properties, combined with its electron-deficient nature and good electron accepting ability, have led to many potential applications in organic light-emitting diodes (OLEDs). Various structural forms as core moiety such as low molecular weight[1b,2] dendrimers[3] and polymers[4] have been studied. Numerous examples of oxadiazole-based compounds have been applied as electron-transporting materials[1b,2] in OLEDs. Most applications were focused on its electron-transporting capability[1b,2] or photoconductivity for advanced electronic devices. Non-mesogenic 2,5-bis(4-naphthyl)-1,3,4-oxadiazole[5] was found to be one of the best organic electron conductors.

On the other hand, examples of 1,3,4-oxadiazole[6] or 1,3,4-thiadiazole[7] derivatives exhibiting mesomorphic properties were rarely reported. 1,3,4-Oxadiazole derivatives were in fact considered as non-linear structures,[8] therefore, reducing the molecular symmetry would possibly lead to a lowering of melting or/and clearing points.[9] This was indeed observed in our previous studies[10] of mesogenic 1,3,4-oxadiazoles. 1,3,4-Oxadiazoles have also been linked to the pyridinium or fluorinated moiety to obtain ionic liquid crystals[11] for optoelectronic applications.

However, examples derived from 1,3,4-oxadiazole exhibiting columnar phases[10,12] were still limited. The metal-containing liquid crystals (or metallomesogens),[13] have been explored and studied. Coordination compounds were considered as the largest category among metallomesogenic materials. The two heteroatoms, N and O with free electron pairs could provide active coordination sites for metal ions or/and hydrogen bond acceptors[14] to expand polymeric frameworks. Non-mesogenic metal complexes[15] such as those of Ag,[16] Ru or Cu were known. Earlier, we described a series of palladium complexes[17] derived from 1,3,4-oxadiazoles exhibiting columnar phases, and found most of them were room temperature liquid crystals. On the other hand, 1,3,4-thiadiazole has a core structure similar to 1,3,4-oxadiazole, different only in the oxygen atom being replaced by sulfur atom. In addition, a less overall bent

* Corresponding author. Tel.: +886 03 4259207; fax: +886 03 4277972.; e-mail: cklai@cc.ncu.edu.tw

0040–4020/$ - see front matter © 2007 Elsevier Ltd. All rights reserved.
doi:10.1016/j.tet.2007.09.031

molecular structure of 1,3,4-thiadiazole was considered. Sulfur atom is slightly larger in size and also more polarized than oxygen atom. In this work, we report the preparation and mesomorphic studies of a new series of copper(II) complexes **1** derived from unsymmetric 1,3,4-thiadiazole. These complexes were considered as rod-like in shape, and they all formed N, SmA or SmC phases. The mesophases formed by derivatives **2** and **3** were probably attributed to the H-bondings induced both intermolecularly or/and intermolecularly by amide (–NH) and phenolic (–OH) groups.

2. Results and discussion

2.1. Synthesis

Two synthetic routes[18] were applied to prepare 1,3,4-oxadiazole derivatives. In this work the synthetic procedures of 2-(5-(2-(alkoxy) naphthalen-6-yl)-1,3,4-thiadiazol-2-yl)-phenols **2** and their copper complexes **1** are given in Scheme 1. The 1,3,4-thiadiazole derivatives **2** were obtained by condensation reaction[17] of hydrazides **3** and P_2S_5 (8.0 equiv) in refluxing pyridine. All derivatives were isolated as white solids or pastes depending on the carbon length attached. Copper complexes were obtained by reactions of 1,3,4-thiadiazoles and $Cu(OAc)_2$ in refluxing $CHCl_3$. The products were recrystallized from CH_2Cl_2/CH_3OH with yields ranging from 74 to 85%. The complexes were also characterized by FTIR spectroscopy and elemental analysis.

2.2. Mesomorphic properties of compounds 2 and 3

The mesomorphic properties of compounds **1**, **2**, and **3** were characterized and investigated by differential scanning calorimetry and polarizing optical microscopy. The phase transitions and thermodynamic data of compounds **3** are listed in Table 1. All compounds **3** except for three derivatives with *no* lateral chain (R_1, R_2=H in Scheme 1) attached on either end of the molecules (n=0 or m=0) formed mesogenic phases. Both the melting and clearing temperatures were insensitive to the length of the side chains. This indicated that the core–core interaction might be the controlling force than van der Waal force in forming the mesophase in this type of amide derivatives. The melting temperatures and clearing

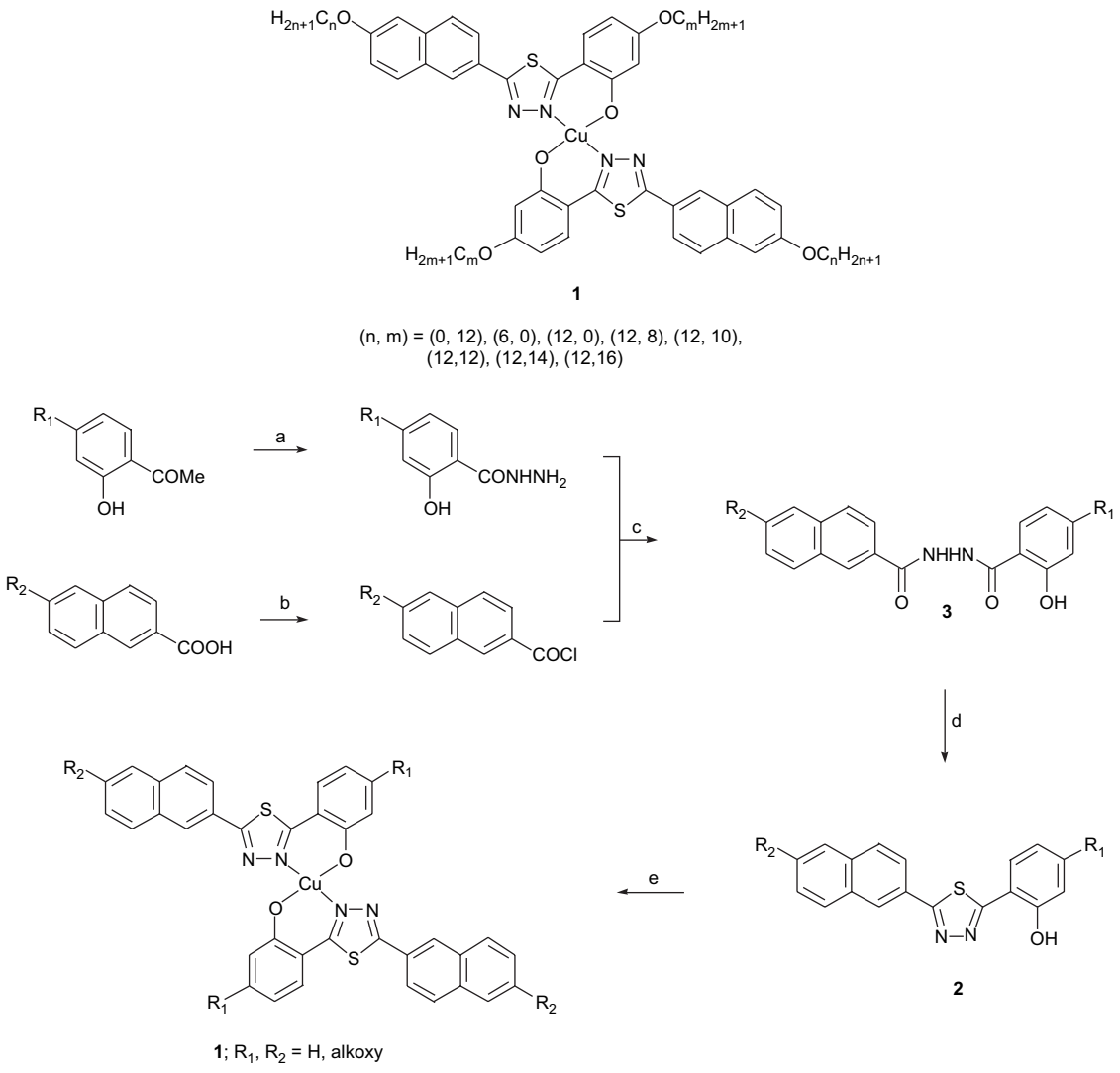

Scheme 1. Reactions and reagents: (a) N_2H_4 (10.0 equiv), refluxing in CH_3OH, 48 h, 90%; (b) $SOCl_2$ (10.0 equiv), refluxing in THF, 1.5 h, 95%; (c) triethylamine (1.0 equiv), stirred in THF at rt, 70%; (d) P_2S_5 (8.0 equiv), refluxing in pyridine, 72 h, 65%; (e) $Cu(OAc)_2$ (0.5 equiv), refluxing in $CHCl_3$, 6 h, 70%.

Table 1. Phase transitions and enthalpies[a] of compounds **3**

	n	*m*	
3	0	12	Cr $\underset{151.9(46.9)}{\overset{166.1(49.1)}{\rightleftharpoons}}$ I
	6	0	Cr $\underset{168.4(32.0)}{\overset{176.7(33.0)}{\rightleftharpoons}}$ I
	12	0	Cr $\underset{167.8(33.9)}{\overset{179.9(33.9)}{\rightleftharpoons}}$ I
	12	8	Cr $\underset{135.1(25.6)}{\overset{153.9(32.3)}{\rightleftharpoons}}$ SmC $\underset{196.7(7.74)}{\overset{199.6(8.29)}{\rightleftharpoons}}$ I
	12	10	Cr $\underset{128.3(23.2)}{\overset{161.8(27.8)}{\rightleftharpoons}}$ SmC $\underset{192.6(6.27)}{\overset{200.9(7.01)}{\rightleftharpoons}}$ I
	12	12	Cr $\underset{130.8(30.3)}{\overset{150.9(36.8)}{\rightleftharpoons}}$ SmC $\underset{193.1(8.98)}{\overset{195.8(9.82)}{\rightleftharpoons}}$ I
	12	14	Cr $\underset{129.1(24.7)}{\overset{152.2(35.4)}{\rightleftharpoons}}$ SmC $\underset{189.9(7.45)}{\overset{192.2(7.90)}{\rightleftharpoons}}$ I
	12	16	Cr $\underset{127.0(25.7)}{\overset{149.9(31.0)}{\rightleftharpoons}}$ SmC $\underset{183.3(7.05)}{\overset{186.2(8.17)}{\rightleftharpoons}}$ I

[a] *n*, *m* represent the carbon numbers in the alkoxy chains. Cr=crystal phases; SmC=smectic C phase; I=isotropic. The transition temperatures (°C) and enthalpies (in parenthesis, kJ/mol) are determined by DSC.

temperatures all ranged between 149.9 and 161.8 °C, and 186.2 and 200.9 °C on heating, respectively. The temperatures of the mesophases ranged from 36.3 to 45.7 °C The phase was characterized and identified as smectic C phase. A typical Schlieren texture under polarizing microscopy was observed when cooled from isotropic liquid. This phase behavior was also consistent with no observation of homeotropic domain. A higher enthalpy (ΔH=7.01–9.82 kJ/mol) for the transition of SmC→I phase was obtained. The SmC phase was also confirmed by powder XRD experiments.

The phase transitions of compounds **2** are listed in Table 2. All compounds **2** except for one derivative (*n*=0, *m*=12) were mesogenic. Interestingly, two other derivatives (*n*=6, *m*=0 and *n*=12, *m*=0), having either a shorter or an identical molecular length were in fact mesogenic. This result indicated that the mesophase was mainly controlled or influenced by the relative carbon length attached on the naphthalene over phenolic ring. On the other hand, the formation of mesophase might be facilitated by the weak π–π interaction between the two neighboring naphthalene rings. This indeed was supported in the crystallographic analysis of compound **2** (*n*=6, *m*=0), and a distance of 3.56 Å between two layers was obtained. These two derivatives (*n*=6, *m*=0 and *n*=12, *m*=0) formed smectic A phases with a short temperature range (ΔT=14.5–33.7 °C on heating) of mesophase. The derivative (*n*=6, *m*=0), the shortest overall molecular length in the series has the narrowest range (ΔT=14.5 °C) of phase temperature. The phase was confirmed and identified as smectic A phase. A fan texture with homeotropic states under polarizing microscopy was observed when cooled from isotropic liquid. The more ordered phase, SmC appeared when the molecular length increased (i.e., *m* or *n* increases). Both the melting and clearing temperatures decreased as carbon length increases. The melting temperatures and clearing temperatures ranged between 153.4 and 144.6 °C, and 217.9 and 198.5 °C on heating, respectively. The temperature range of the

Table 2. Phase transitions and enthalpies[a] of 1,3,4-thiodiazole derivatives **2**

	n	*m*	
2	0	12	Cr $\underset{153.8(32.3)}{\overset{173.9(44.1)}{\rightleftharpoons}}$ I
	6	0	Cr $\underset{164.3(40.8)}{\overset{183.3(41.0)}{\rightleftharpoons}}$ SmA $\underset{196.1(5.63)}{\overset{197.8(5.55)}{\rightleftharpoons}}$ I
	12	0	Cr $\underset{144.6(42.9)}{\overset{161.2(44.6)}{\rightleftharpoons}}$ SmA $\underset{190.9(5.61)}{\overset{194.9(5.66)}{\rightleftharpoons}}$ I
	12	8	Cr $\underset{143.6(45.7)}{\overset{153.4(45.2)}{\rightleftharpoons}}$ SmC $\underset{213.1(0.09)^b}{\overset{213.1(0.30)^b}{\rightleftharpoons}}$ SmA $\underset{216.6(4.44)^b}{\overset{217.9(5.42)^b}{\rightleftharpoons}}$ I
	12	10	Cr $\underset{136.9(43.2)}{\overset{150.3(44.8)}{\rightleftharpoons}}$ SmC $\underset{210.6(7.51)}{\overset{212.9(7.59)}{\rightleftharpoons}}$ I
	12	12	Cr $\underset{129.9(45.2)}{\overset{148.1(45.7)}{\rightleftharpoons}}$ SmC $\underset{201.9(7.45)}{\overset{204.2(7.54)}{\rightleftharpoons}}$ I
	12	14	Cr $\underset{127.6(50.4)}{\overset{144.1(51.6)}{\rightleftharpoons}}$ SmC $\underset{200.6(8.08)}{\overset{201.7(8.16)}{\rightleftharpoons}}$ I
	12	16	Cr $\underset{118.7(36.7)}{\overset{144.6(38.8)}{\rightleftharpoons}}$ SmC $\underset{194.2(5.85)}{\overset{198.5(6.14)}{\rightleftharpoons}}$ I

[a] *n*, *m* represent the carbon numbers in the alkoxy chains. Cr=crystal phases; SmA=smectic A; SmC=smectic C phase; I=isotropic. The transition temperatures (°C) and enthalpies (in parenthesis, kJ/mol) are determined by DSC.
[b] Determined by DSC at a scan rate of 5.0 °C/min.

mesophases ranged from 62.6 (*n*=12, *m*=10) to 45.7 °C (*n*=12, *m*=16) on heating. A higher enthalpy (ΔH=6.14–8.16 kJ/mol) for the transition of SmC→I phase was also obtained. The H-bondings induced by amide (–NH)[21] or/and phenolic (–OH) group might be attributed to the formation of the mesophase observed in compounds **2** and **3**.

2.3. Mesomorphic properties of compounds 1

The phase transition thermodynamic data of copper complexes **1** are summarized in Table 3. All copper complexes were slightly decomposed upon heating above their clearing temperatures. All compounds **1** formed mesogenic phases, and the phases were identified as N, SmA or/and SmC phases depending on the carbon length. The overall molecular length of the copper complexes **1** increased upon coordination with copper ion, therefore, the melting and the clearing temperatures were all increased by ca. 40.7–70.1 °C and 60.0–70.8 °C, respectively. Both the melting and clearing temperatures were slightly decreased with carbon chain lengths. The melting temperatures and clearing temperatures of compounds **1** ranged between 200.9 and 253.4 °C, and 258.5 and 278.5 °C on heating, respectively. The temperature range of the mesophases ranged from 12.3 to 62.4 °C. The derivative (*n*=6, *m*=0), with the shortest overall molecular length exhibited N phase with the narrowest range (ΔT=12.3 °C). The phases were characterized and identified as N, SmA and SmC phases based on the textures observed by optical microscope (Fig. 1).

2.4. Single crystal structure of 2-(5-(2-(hexyloxy)-naphthalene-6-yl)-1,3,4-thiadiazol-2-yl) phenol 2 (*n*=6, *m*=0)

A single crystal isolated as brown needle of mesogenic compound **2** (*n*=6, *m*=0) suitable for X-ray diffraction analysis

Table 3. Phase transitions and enthalpies[a] of copper complexes **1**

	n	*m*	
1	0	12	$\mathrm{Cr} \underset{213.1(27.9)}{\overset{231.7(32.4)}{\rightleftharpoons}} \mathrm{SmA} \underset{264.0^{b}}{\overset{278.5(1.83)}{\rightleftharpoons}} \mathrm{I_d}$
	6	0	$\mathrm{Cr} \underset{184.7(17.1)}{\overset{253.4(66.7)}{\rightleftharpoons}} \mathrm{N} \underset{250.0^{b}}{\overset{265.7(0.37)}{\rightleftharpoons}} \mathrm{I_d}$
	12	0	$\mathrm{Cr} \underset{180.9(23.2)}{\overset{201.9(59.7)}{\rightleftharpoons}} \mathrm{SmA} \underset{261.0^{b}}{\overset{264.3(5.88)}{\rightleftharpoons}} \mathrm{I_d}$
	12	8	$\mathrm{Cr} \underset{\mathrm{SmC}\ 218.0^{b}}{\overset{225.7\ (38.4)}{\rightleftharpoons}} \mathrm{SmA} \underset{272.0^{b}}{\overset{279.0^{b}}{\rightleftharpoons}} \mathrm{I_d}$
	12	10	$\mathrm{Cr} \underset{203.8(40.4)}{\overset{219.7(47.7)}{\rightleftharpoons}} \mathrm{SmC} \underset{263.0^{b}}{\overset{276.0(12.1)}{\rightleftharpoons}} \mathrm{I_d}$
	12	12	$\mathrm{Cr} \underset{205.0(40.2)}{\overset{215.5(45.8)}{\rightleftharpoons}} \mathrm{SmC} \underset{260.0^{b}}{\overset{265.3(9.32)}{\rightleftharpoons}} \mathrm{I_d}$
	12	14	$\mathrm{Cr} \underset{199.0(38.5)}{\overset{209.3(42.9)}{\rightleftharpoons}} \mathrm{SmC} \underset{250.0(0.33)}{\overset{262.7(8.65)}{\rightleftharpoons}} \mathrm{I_d}$
	12	16	$\mathrm{Cr} \underset{289.6(13.7)}{\overset{200.9(32.9)}{\rightleftharpoons}} \mathrm{SmC} \underset{250.0^{b}}{\overset{258.5(20.9)}{\rightleftharpoons}} \mathrm{I_d}$

[a] *n*, *m* represent the carbon numbers in the alkoxy chains. Cr=crystal phases; SmA=smectic A; SmC=smectic C; N=nematic phase; I_d=isotropic with slight decomposition. The transition temperatures (°C) and enthalpies (in parenthesis, kJ/mol) are determined by DSC.
[b] Obtained by optical microscope.

was slowly grown from CH_2Cl_2/CH_3OH solution at room temperature, and the crystal structure was investigated. Figure 2 shows the molecular structure with the atomic numbering scheme. When viewed from the side, the three planes of thiadiazole, naphthalene, and benzene were nearly coplanar, and this coplanar structure might facilitate the molecular arrangement and the formation of the mesophases. The overall molecular shape is slightly bent, and the overall length and the width of the molecule are measured to be ca. 22.32 Å and 3.74 Å. There are two molecules existing in the unit cell, and the molecules are all tilted. The molecules are arranged anti-parallel within the neighboring layers. A perpendicular distance between the intermolecular benzenes within the layers is measured as ca. 3.56 Å (Fig. 3), indicating that a very weak π–π interaction is possibly existent. Interestingly, the crystallographic data indicated that the phenolic-H atom (–OH) was conformationally located or pointed out to the other side of the N1 and N2 atoms of the thiadiazole ring and also at trans position away from sulfur atom of the thiadiazole ring. Therefore, an intramolecular H-bonding between S(1) and H–O(1) atoms was not possibly formed at room temperature. On the other hand, an intermolecular H-bonding distance of 1.89 Å between N2 and H1A atoms was observed, and its angle defined by O1, H1A, and N2 atoms was measured to be 161.5°. This molecular arrangement is consistent with the layer structures observed by powder XRD and optical textures. A variable temperature XRD experiment for compounds was also performed to confirm the structure of the mesophases. A diffraction pattern with two peaks for compound **2** (*n*=6, *m*=0) at *d*-spacings of 34.42 Å and 17.22 Å was obtained (Fig. 4). The two peaks corresponded to the layer indices 001 and 002. A tilted angle in the smectic phase was roughly calculated as ~59° by *d*-spacing value and the molecular length (ca. 40.06 Å, obtained from MM2 simulation).

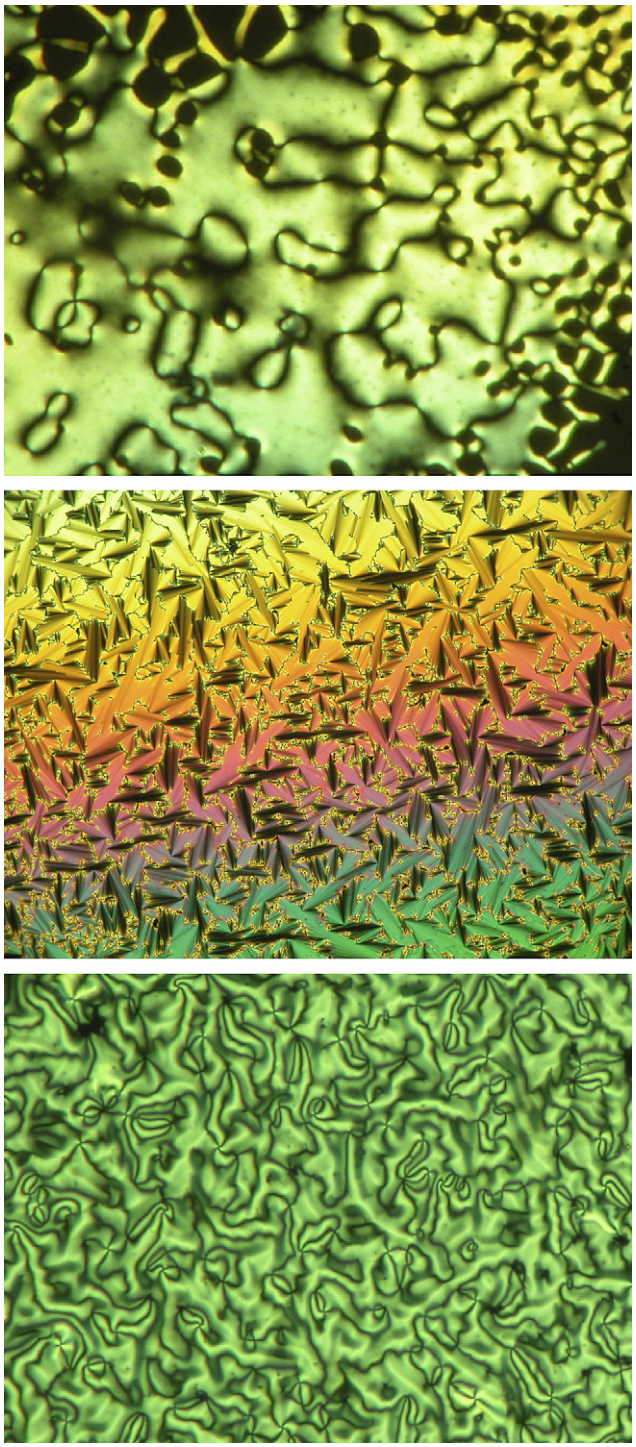

Figure 1. The optical textures observed in compounds. Top plate: N phase by **1** (*n*=6, *m*=0) at 243 °C, center plate: SmA phase by **1** (*n*=12, *m*=0) at 235 °C, and bottom plate: SmC phase by **1** (*n*=12, *m*=10) at 227 °C.

2.5. Studies of H-bonding formation by ^{1}H NMR and FTIR spectroscopies

In this work we compare ^{1}H NMR spectroscopic data as a function of concentration. In a typical experiment, a 0.1 mM solution of compound **2** (*n*=6, *m*=0) was prepared by dissolving a sample in $CDCl_3$ in order to reduce the molecular attraction.[19] A sharp singlet occurred at 11.475 ppm, assigned to phenolic –OH group was monitored, and this

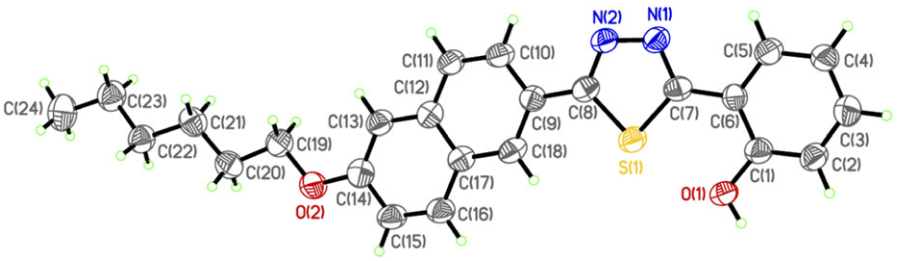

Figure 2. An ORTEP plot for compound **2** (n=6, m=0) with the numbering scheme, and the thermal ellipsoids of the non-hydrogen atoms are drawn at the 50% probability level. Parameters: triclinic; space group P-1; a=7.4255(18) Å, b=8.209(2) Å, c=17.315(5) Å; α=101.245(13)°, β=92.501(13)°, γ=95.804(17)°; Z=2; density (calcd)=1.307 Mg/m^3.

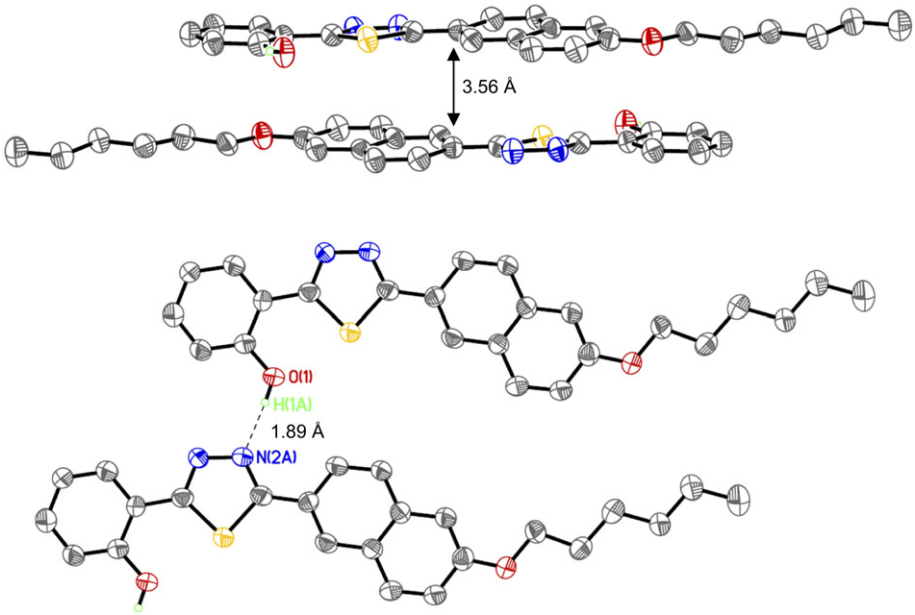

Figure 3. The weak π–π interaction between the layers (top) and the H-bonding (bottom) in compound **2** (n=6, m=0).

characteristic peak was not shifted upfield when dissolved in more concentrated solution (3 orders of magnitude). The concentration independence indicated that the H-bondings are quite stable. The *intermolecular* H-bondings observed in single crystallographic state might convert to *intramolecular* H-bondings in solution state due to an increased distance. Also the –OH signal was found to have no correlation with concentration.

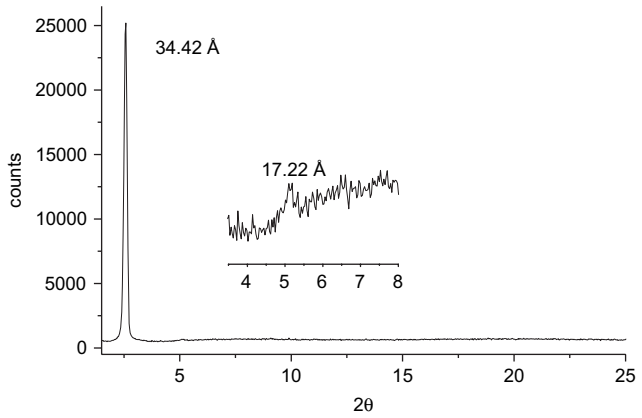

Figure 4. X-ray powder diffraction pattern of compound **2** (n=6, m=0) at 180 °C.

When a more polar solvent, DMSO-d_6 was added,[19b,20] the characteristic phenolic peak started to appear upfield, i.e., δ=11.475 ($CDCl_3$-d_1/DMSO-d_6: 1/0)→δ=11.354 (9/1)→δ=11.097 (5/1), shown in Figure 5. In addition, the signal started to broaden. However, as the ratio of $CDCl_3$-d_1/DMSO-d_6 was increased to 1/1, the peak was shifted to δ=10.779. The $\Delta\delta$=0.696 then reached the maximum. The upfield shifting and the peak broadening were no longer observed, and the peak was barely observed. The result indicated that *intermolecular* H-bondings were indeed existent, which might be explained as follows. The oxygen atom on the DMSO has a higher electron density and is a stronger electron donor. On the other hand, hydrogen atom of the phenolic group in compound **2** (n=6, m=0) carries a partial positive charge. A dipole–dipole interaction ($\delta^+\cdots\delta^-$) occurred upon the addition of DMSO, which caused the electron density enhancement on the hydrogen atom. The original H-bondings were destroyed, and the signal appeared *upfield*. Nevertheless, the characteristic signal which appeared broader was attributed to the fast proton exchange.[21]

In order to confirm the H-bondings formed in crystal, liquid crystal or/and isotropic state by compounds **2**, variable temperature FTIR spectra[7b,22] of thin films were studied. In general, the IR frequency of *intermolecular* H-bondings

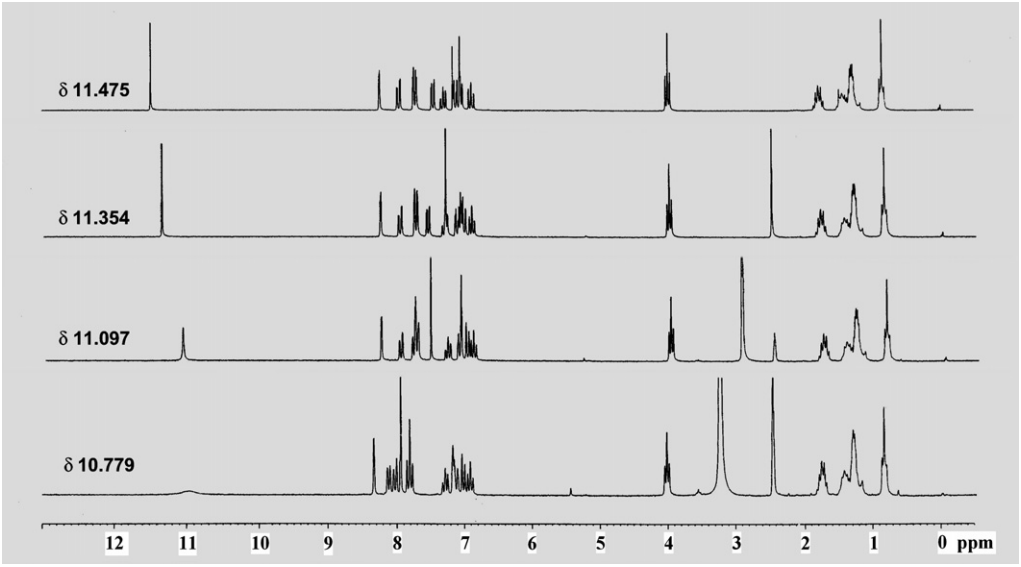

Figure 5. Plots of ^{1}H NMR spectra observed for compound **2** (n=6, m=0) dissolved in $CDCl_3$-d_1/DMSO-d_6 with a ratio of (a) 1/0 (top) (b) 9/1 (c) 5/1 (d) 1/1 (bottom).

by phenolic –OH group[22e,23] occurred at ca. 3200–3400 cm^{-1}, and *intramolecular* H-bondings then occurred at lower region[24] of 2800–3100 cm^{-1}. As seen from Figure 6, a characteristic peak of *intramolecular* H-bondings which occurred at ca. 3029 cm^{-1}, assigned to the phenolic –OH group was not found to shift with temperature. However, the total band area was decreased. This indicated that an *intramolecular* H-bonding in compounds **2** was existent in crystal, liquid crystal and isotropic states.

2.6. Optical properties

1,3,4-Oxadiazoles have been investigated as an excellent candidate for light-emitting materials due to their photophysical and fluorescent properties. The UV–vis absorption spectra for compounds **1** and **2** in CH_2Cl_2 solution are presented in Figure 7. All compounds **2** exhibited a unique intense absorption λ_{max} peak at 363 nm except for compound **2** (n=12, m=0) which occurred at 359 nm, and these absorption spectra were very similar in shape because of their structural similarity. The highest absorption peaks of all compounds were not sensitive to the carbon length or/and number of terminal chains. These absorption spectra corresponded to the transitions of $n\rightarrow\pi^*$ and $\pi\rightarrow\pi^*$. The emission luminescence spectra of compounds **2** measured in CH_2Cl_2 are shown in Figure 7. A similar trend was observed in the photoluminescence spectra. The emission peaks occurred at 519–537 nm. The solution PL spectra were quite similar in peak shape to UV–vis spectra except for compound **2** (n=12, m=0). Compound **2** (n=12, m=0) with no electron donating group on the phenyl group has an absorption peak red-shifted by ca. 18–23 nm. On the other hand, all the other three derivatives n=12, m=8; n=12, m=12; n=12, m=16 were considered as electron withdrawing groups and were then blue-shifted to the lower frequencies. However, the quantum yields in CH_2Cl_2 were relatively low.

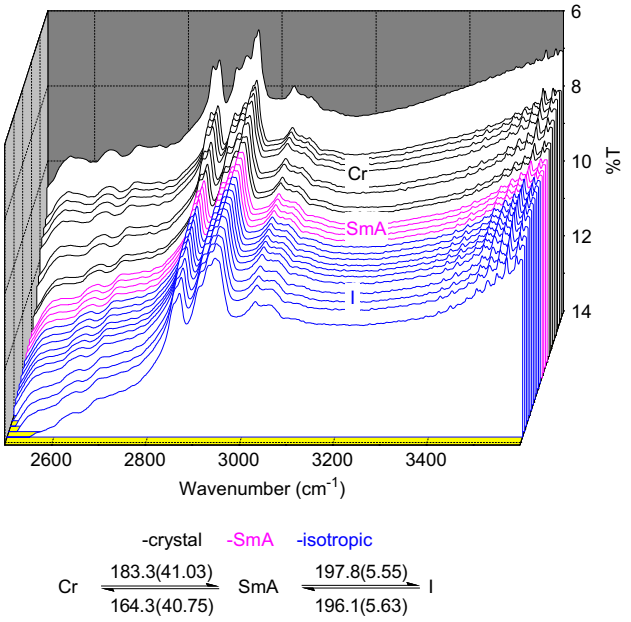

Figure 6. Variable temperature FTIR spectra of compound **2** (n=6, m=0) obtained during cooling process at a scan rate of 5.0 °C/min.

The PL spectra of compounds **2** (Fig. 7b) showed two intense peaks, which were attributed to the excited state intramolecular proton transfer[23,25] (ESIPT). A longer wavelength emitted by an excited phototautomer form than by an excited normal form was often observed. The Stokes shift values were found to be as large as 6000–12,000 cm^{-1} for many ESIPT compounds. The ESIPT reactions have been known to occur in a variety of oxadiazole derivatives,[22a] as well as other related compounds, such as *ortho*-hydroxybenzaldehydes, acetophenones, etc. Unfortunately, the noticeable quenching of fluorescence has largely restricted the practical applications of this type of organic materials. In our system, the ESIPT reaction was enhanced or/and facilitated by an *intramolecular* H-bonding. The two phototautomer forms, enol and keto coexisting in the excited state, were attributed to the two emission peaks on the PL spectra. The enol form emitted light at a lower wavelength, while keto form emitted light at higher wavelength. Without the ESIPT reactions the

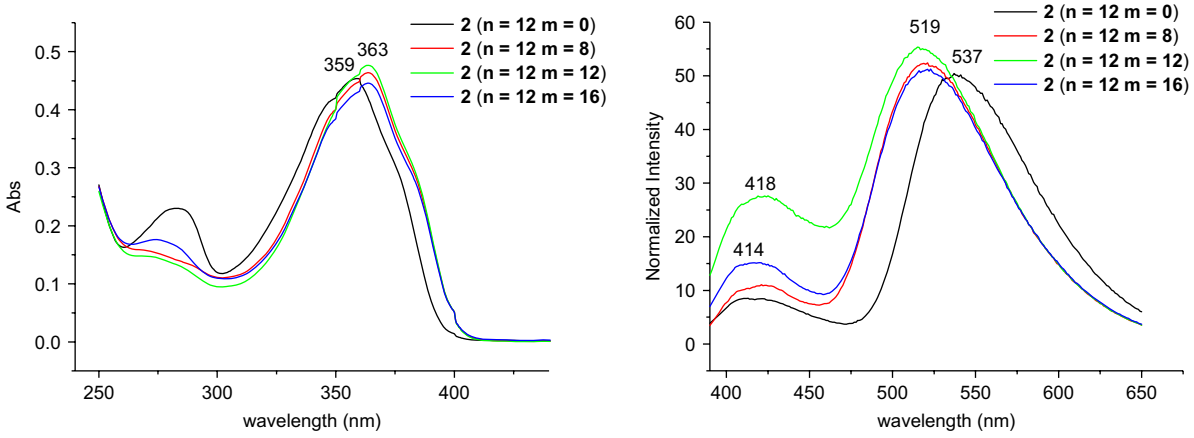

Figure 7. Normalized UV and PL spectra of compounds **2** in CH_2Cl_2 at 25 °C.

enol form returned directly to the ground state ($S_1 \rightarrow S_0$) by emitting a shorter wavelength light, and keto form then underwent a large Stokes shift. On the other hand, the ESIPT molecules generated in the excited state transferred to the lower energy state ($S_1 \rightarrow S_1'$), which were accompanied by emission of the fluorescent light in a higher wavelength.[26]

3. Conclusions

A new series of heterocyclic 1,3,4-thiadiazoles **2** and copper complexes **1** as core group are prepared and their mesomorphic properties investigated. The precursors **3** and **2** formed SmC or/and SmA phases; however, copper complexes **1** formed N, SmA or/and SmC phases. The temperature range of the mesophases formed by 1,3,4-oxadiazoles **2** and copper complexes **1** remained about the same. The X-ray single crystallographic analysis indicated that compounds **2** formed an *intermolecular* H-bonding in single crystalline state. However, an *intramolecular* H-bonding was observed in crystalline state, smectic phase and isotropic states, which were also supported by FTIR spectra. Optical properties evaluated for potential light-emitting materials were studied, in which ESIPT reactions were observed in this system.

4. Experimental

4.1. General

^1H and ^{13}C NMR spectra were measured on a Bruker DRS-200 spectrometer. DSC thermographs were obtained on a Mettler DSC 822. All phase transitions are determined at a scan rate of 10.0 °C/min. Optical polarized microscopy was carried out on Zeiss Axioplan 2 equipped with a hot stage system of Mettler FP90/FP82HT. The UV–vis absorption and fluorescence spectra were obtained using JASCO V-530 spectrometer and HITACHI F-4500 spectrophotometer. Elemental analyses for carbon, hydrogen, and nitrogen were conducted at Instrumentation Center, National Taiwan University on a Heraeus CHN-O-Rapid elemental analyzer. Data for all X-ray structures were collected using a BRUKER SMART CCD diffractometer with graphite-monochromated Mo Kα radiation (λ=0.71073 Å) at 150±1 K. The structure was solved by direct methods and refined by full matrix least-squares and difference Fourier techniques with SHELXTL. Empirical absorption corrections were applied with SADABS program. All non-hydrogen atoms were refined anisotropically. The powder diffraction data were collected from the Wiggler-A beam line of the National Synchrotron Radiation Research Center with the wavelength of 1.3263 Å. Methyl 4-alkoxy-2-hydroxybenzoates and 4-alkoxy-2- hydroxybenzoic acid hydrazides were prepared by literature methods.[17]

4.2. 6-Dodecyloxy-naphthalene-2-carboxylic acid (*n*=12)

The mixture of 6-hydroxy-2-naphthoic acid (10.0 g, 0.053 mol), 1-bromododecane (13.21 g, 0.053 mol), and KOH (5.95 g, 0.106 mol) was dissolved in 250 mL of C_2H_5OH (95%), and the solution was refluxed for 24 h. The solution was cooled and neutralized with dilute HCl (1.5 M). The solvent was removed under vacuum, and the white solids were collected. The solids were dissolved in 50 mL of CH_2Cl_2 and then extracted twice with water. The organic layers were combined and dried over $MgSO_4$. The products, isolated as white solids, were obtained after recrystallization from CH_2Cl_2/CH_3OH. Yield 78%. ^1H NMR ($CDCl_3$): δ 0.87 (t, 3H, $-CH_3$, J=6.69 Hz), 1.26–1.50 (m, 18H, $-CH_2$), 1.78–1.84 (m, 2H, $-OCH_2CH_2$), 4.09 (t, 2H, $-OCH_2$, J=6.53 Hz), 7.13 (s, 1H, $-C_{10}H_6$), 7.16 (d, 1H, $-C_{10}H_6$, J=11.34 Hz), 7.70 (d, 1H, $-C_{10}H_6$, J=8.64 Hz), 7.81 (d, 1H, $-C_{10}H_6$, J=8.97 Hz), 7.99 (d, 1H, $-C_{10}H_6$, J=10.12 Hz), 8.49 (s, 1H, $-C_{10}H_6$). ^{13}C NMR ($CDCl_3$): δ 13.92, 22.58, 26.05, 28.84, 29.17, 29.25, 29.32, 29.47, 29.52, 29.57, 31.85, 68.26, 106.68, 119.76, 125.66, 125.88, 126.64, 127.92, 130.65, 130.74, 137.21, 159.11, 166.90.

4.3. 6-(Dodecyloxy)naphthalene-2-carboxylic acid *N*-(4-(dodecyloxy)-2-hydroxybenzoyl)hydrazide (3; *n*=12, *m*=12)

The mixture of 6-(dodecyloxy)naphthalene-2-carboxylic acid (1.5 g, 0.42 mmol) and $SOCl_2$ (3.0 mL, 0.084 mol) dissolved in 3.0 mL of dry THF was refluxed for 1 h under nitrogen atmosphere. The excess $SOCl_2$ and THF were removed under reduced pressure. The solids was redissolved in 15 mL of dried THF, and transferred to a three-necked flask. The solution was cooled in an ice bath for further reaction. The three-necked flask was connected to two

addition funnels. The first funnel was charged with a solution of methyl 4-dodecyloxy-2-hydroxybenzoic acid hydrazide (1.42 g, 0.42 mmol) dissolved in 25 mL of dry THF, and the second funnel was filled with a solution of TEA (0.86 g, 0.84 mmol) dissolved in 20 mL of dry THF. Both solutions in the two funnels were added dropwise to the acid chloride solution at ice bath temperature. The solution was stirred for 4 h. Water was poured to the solution, and solids were collected. The products, isolated as white solids, were obtained after recrystallization from CH_2Cl_2/MeOH. Yield 70%. ^{1}H NMR ($CDCl_3$): δ 0.86–0.89 (m, 6H, –CH_3), 1.27–1.50 (m, 40H, –CH_2), 1.77–1.87 (m, 4H, –OCH_2CH_2), 3.98 (t, 2H, –OCH_2, J=6.55 Hz), 4.10 (t, 2H, –OCH_2, J=6.53 Hz), 6.45–6.47 (m, 2H, –C_6H_3), 7.15 (s, 1H, –$C_{10}H_6$), 7.21 (d, 1H, –$C_{10}H_6$, J=11.35 Hz), 7.43 (d, 1H, –$C_{10}H_6$, J=9.45 Hz), 7.77–7.83 (m, 3H, Ar–H), 8.31 (s, 1H, –$C_{10}H_6$), 9.01 (s, 1H, –NH), 9.09 (s, 1H, –NH), 11.54 (s, 1H, –OH). ^{13}C NMR ($CDCl_3$): δ 13.94, 22.59, 25.92, 26.05, 29.00, 29.15, 29.26, 29.27, 29.33, 29.48, 29.51, 29.53, 29.56, 29.58, 31.85, 68.31, 68.39, 102.37, 105.08, 106.71, 108.00, 120.36, 123.61, 125.99, 126.83,127.43, 127.94, 127.98, 130.51, 137.00, 158.12, 159.21, 163.73, 164.79, 166.38. Anal. Calcd for $C_{42}H_{62}N_2O_5$: C 74.74, H 9.26, N 4.15. Found: C 74.52, H 9.25, N 4.13.

4.4. 2-Naphthoic acid *N*-(4-(dodecyloxy)-2-hydroxybenzoyl)hydrazide (3; *n*=0, *m*=12)

White solid, yield 63%. ^{1}H NMR ($CDCl_3$): δ 0.88 (t, 3H, –CH_3, J=4.57 Hz), 1.27–1.53 (m, 18H, –CH_2), 1.73–1.79 (m, 2H, –OCH_2CH_2), 3.93 (t, 2H, –OCH_2, J=6.53 Hz), 6.38–6.39 (m, 2H, –$C_{10}H_7$), 7.51–7.58 (m, 3H, Ar–H), 7.84–7.90 (m, 4H, Ar–H), 8.38 (s, 1H, –$C_{10}H_7$), 9.23 (s, 1H, –NH), 9.52 (s, 1H, –NH), 11.49 (s, 1H, –OH). ^{13}C NMR ($CDCl_3$): δ 13.89, 22.56, 25.91, 29.01, 29.23, 29.27, 29.47, 29.50, 29.54, 29.56, 31.84, 68.35, 102.37, 105.25, 107.85, 123.15, 126.95, 127.23, 127.76, 128.13, 128.28, 128.51, 128.74, 129.05, 132.62, 135.27, 159.21, 163.54, 164.77, 167.10. Anal. Calcd for $C_{30}H_{38}N_2O_4$: C 73.44, H 7.81, N 5.71. Found: C 73.27, H 7.78, N 5.68.

4.5. 6-(Dodecyloxy)naphthalene-2-carboxylic acid *N*-(2-hydroxybenzoyl)hydrazide (3; *n*=12, *m*=0)

White solid, yield 79%. ^{1}H NMR ($CDCl_3$): δ 0.88 (t, 3H, –CH_3, J=4.48 Hz), 1.16–1.52 (m, 18H, –CH_2), 1.82–1.88 (m, 2H, –OCH_2CH_2), 4.09 (t, 2H, –OCH_2, J=6.48 Hz), 6.85 (d, 1H, –$C_{10}H_6$, J=7.50 Hz), 6.95 (d, 1H, Ar–H, J=8.35 Hz), 7.13–7.20 (m, 2H, Ar–H), 7.38 (s, 1H, –$C_{10}H_6$), 7.62 (d, 1H, –$C_{10}H_6$, J=7.85 Hz), 7.73–7.83 (m, 3H, Ar–H), 8.30 (s, 1H, –$C_{10}H_6$), 9.19 (s, 1H, –NH), 9.76 (s, 1H, –NH), 11.21 (s, 1H, –OH). ^{13}C NMR ($CDCl_3$): δ 13.89, 22.56, 26.04, 29.15, 29.23, 29.31, 29.51, 29.54, 29.56, 31.83, 68.35, 106.79, 112.58, 118.54, 119.20, 120.34, 123.62, 125.86, 127.42, 127.93, 128.12, 130.52, 134.84, 137.06, 159.28, 161.17, 164.96, 166.60. Anal. Calcd for $C_{30}H_{38}N_2O_4$: C 73.44, H 7.81, N 5.71. Found: C 73.39, H 7.83, N 5.70.

4.6. 5-(Dodecyloxy)-2-(5-(2-(dodecyloxy)naphthalen-6-yl)-1,3,4-thiadiazol-2-yl)phenol (2; *n*=12, *m*=12)

The mixture of 6-(dodecyloxy)naphthalene-2-carboxylic acid *N*-(4-(dodecyloxy)-2-hydroxy benzoyl)hydrazide (1.20 g, 1.80 mmol) and P_2S_5 (3.20 g, 14.4 mol) was dissolved in 20.0 mL of pyridine. The solution was refluxed for 48 h. The solution was then extracted with CH_2Cl_2 and washed with aqueous KOH. The organic layers were collected and washed again with aqueous HCl. The organic layers were collected and dried over $MgSO_4$. The products, isolated as pale yellow solids, were obtained after recrystallization from CH_2Cl_2/CH_3OH. Yield 74%. ^{1}H NMR ($CDCl_3$): δ 0.87–0.89 (m, 6H, –CH_3), 1.28–1.51 (m, 40H, –CH_2), 1.77–1.87 (m, 4H, –OCH_2CH_2), 3.98–4.10 (m, 4H, –OCH_2), 6.51 (d, 1H, –C_6H_3, J=10.90 Hz), 6.59 (s, 1H, –C_6H_3), 7.14 (s, 1H, –$C_{10}H_6$), 7.20 (d, 1H, –$C_{10}H_6$, J=11.2 Hz), 7.40 (d, 1H, –$C_{10}H_6$, J=11 Hz), 7.77–7.80 (m, 2H, Ar–H), 8.05 (d, 1H, –$C_{10}H_6$, J=10.00 Hz), 8.29 (s, 1H, –$C_{10}H_6$). ^{13}C NMR ($CDCl_3$): δ 13.90, 22.57, 25.94, 26.05, 29.07, 29.18, 29.24, 29.27, 29.32, 29.47, 29.50, 29.55, 29.57, 31.84, 68.34, 68.41, 76.65, 76.90, 77.15, 102.30, 107.01, 107.59, 108.54, 120.28, 124.79, 124.93, 127.72, 127.96, 128.51, 130.10, 130.68, 136.25, 158.86, 159.40, 163.11, 165.44, 169.29. Anal. Calcd for $C_{42}H_{60}N_2O_3S$: C 74.96, H 8.99, N 4.16. Found: C 74.91, H 9.03, N 4.15.

4.7. 2-(5-(2-(Dodecyloxy)naphthalen-6-yl)-1,3,4-thiadiazol-2-yl)phenol (2; *n*=12, *m*=0)

Light yellow solid, yield 78%. ^{1}H NMR ($CDCl_3$): δ 0.88 (t, 3H, –CH_3, J=4.62 Hz), 1.28–1.52 (m, 18H, –CH_2), 1.84–1.86 (m, 2H, –OCH_2CH_2), 4.09 (t, 2H, –OCH_2, J=6.55 Hz), 6.94 (s, 1H, –C_6H_4), 7.12–7.14 (m, 2H, Ar–H), 7.18–7.21 (m, 1H, –C_6H_4), 7.36 (s, 1H, –$C_{10}H_6$), 7.51 (d, 1H, –$C_{10}H_6$, J=7.76 Hz), 7.77–7.80 (m, 2H, Ar–H), 8.02 (d, 1H, –$C_{10}H_6$, J=9.90 Hz), 8.31 (s, 1H, –OH). ^{13}C NMR ($CDCl_3$): δ 13.89, 22.57, 26.05, 29.18, 29.24, 29.33, 29.50, 29.52, 29.55, 29.58, 31.84, 68.35, 107.01, 114.32, 118.10, 119.79, 120.36, 124.72, 124.81, 127.78, 128.16, 128.49, 129.57, 130.14, 132.56, 136.38, 157.49, 159.00, 166.69, 169.31. Anal. Calcd for $C_{30}H_{36}N_2O_2S$: C 73.73, H 7.43, N 5.73. Found: C 73.51, H 7.53, N 5.67.

4.8. 5-(Dodecyloxy)-2-(5-(naphthalen-2-yl)-1,3,4-thiadiazol-2-yl)phenol (2; *n*=0, *m*=12)

Light yellow solid, yield 70%. ^{1}H NMR ($CDCl_3$): δ 0.89 (t, 3H, –CH_3, J=4.60 Hz), 1.28–1.48 (m, 18H, –CH_2), 1.48–1.81 (m, 2H, –OCH_2CH_2), 3.99 (t, 2H, –OCH_2, J=6.55 Hz), 6.52 (d, 1H, Ar–H, J=11.00 Hz), 6.58 (s, 1H, Ar–H), 7.39 (d, 1H, –$C_{10}H_6$, J=8.65 Hz), 7.53–7.54 (m, 2H, –$C_{10}H_6$), 7.85 (d, 1H, –$C_{10}H_6$, J=5.15 Hz), 7.90–7.92 (m, 2H, Ar–H), 8.07 (d, 1H, –$C_{10}H_6$, J=10.05 Hz), 8.37 (s, 1H, –$C_{10}H_6$), 11.56 (s, 1H, –OH). ^{13}C NMR ($CDCl_3$): δ 13.89, 22.57, 25.94, 29.07, 29.24, 29.28, 29.47, 29.50, 29.55, 29.57, 31.84, 68.42, 102.32, 107.51, 108.60, 124.29, 127.05, 127.25, 127.65, 127.88, 128.13, 128.63, 129.05, 130.72, 133.21, 134.65, 159.46, 163.22, 165.12, 165.12, 169.73. Anal. Calcd for $C_{30}H_{36}N_2O_2S$: C 73.73, H 7.43, N 5.73. Found: C 73.78, H 7.34, N 5.71.

4.9. Bis(5-(dodecyloxy)-2-(5-(2-(dodecyloxy)-naphthalen-6-yl)-1,3,4-thiadiazol-2-yl)phenol) copper(II) (1; *n*=12, *m*=12)

A solution of 5-(dodecyloxy)-2-(5-(2-(dodecyloxy)naphthalen-6-yl)-1,3,4-thiadiazol-2-yl)phenol (0.15 g, 0.22 mmol)

dissolved in 40 mL of $CHCl_3/C_2H_5OH$ (4/1) was added to the solution of copper(II) acetate hydrate (0.022 g, 0.11 mmol) dissolved in 5.0 mL of $CHCl_3$. The solution was refluxed for 4 h. The brown solids were filtered and collected. The products were obtained by recrystallization from CH_2Cl_2/CH_3OH. Yield 84%. Anal. Calcd for $C_{84}H_{118}CuN_4O_6S_2$: C 71.68, H 8.45, N 3.98. Found: C, 71.69, H 8.51, N 3.96. MS (FAB): 1407.4 (MH^+).

Acknowledgements

We thank the National Science Council of Taiwan, ROC (NSC-94-2738-M-008-001) for generous support of this work.

References and notes

1. (a) Schultz, B.; Bruma, M.; Brehmer, L. *Adv. Mater.* **1997**, *9*, 601; (b) Kulkarni, A. P.; Tonzola, C. J.; Babel, A.; Jenekhe, S. A. *Chem. Mater.* **2004**, *16*, 4556; (c) Hughes, G.; Bryce, M. R. *J. Mater. Chem.* **2005**, *15*, 94; (d) Boltona, O.; Kim, J. *J. Mater. Chem.* **2007**, *17*, 1981; (e) Collins, I. *J. Chem. Soc., Perkin Trans. 1* **2000**, 2845.
2. (a) Oyston, S.; Wang, C.; Hughes, G.; Batsanov, A. S.; Perepichka, I. F.; Bryce, M. R.; Ahn, J. H.; Pearson, C.; Petty, M. C. *J. Mater. Chem.* **2005**, *15*, 194; (b) Ichikawa, M.; Kawaguchi, T.; Kobayashi, K.; Miki, T.; Furukawa, T.; Koyamaa, T.; Taniguchi, Y. *J. Mater. Chem.* **2006**, *16*, 221; (c) Strohriegl, P.; Grazulevicius, J. V. *Adv. Mater.* **2002**, *14*, 1439; (d) Hughes, G.; Bryce, M. R. *J. Mater. Chem.* **2004**, *15*, 94; (e) Kamtekar, K. T.; Wang, C.; Bettington, S.; Batsanov, A. S.; Perepichka, I. F.; Bryce, M. R.; Ahn, J. H.; Rabinalb, M.; Petty, M. C. *J. Mater. Chem.* **2006**, *16*, 3823; (f) Wang, C.; Pålsson, L. O.; Batsanov, A. S.; Bryce, M. R. *J. Am. Chem. Soc.* **2006**, *128*, 3789.
3. Cha, S. W.; Choi, S. H.; Kim, K.; Jin, J. I. *J. Mater. Chem.* **2003**, *13*, 1900.
4. (a) Kim, J. H.; Park, J. H.; Lee, H. *Chem. Mater.* **2003**, *15*, 3414; (b) Lee, D. W.; Kwon, X. Y.; Jin, J. I.; Park, Y.; Kim, Y. R.; Hwang, L. W. *Chem. Mater.* **2001**, *13*, 565; (c) Lee, Y. X.; Chen, X.; Chen, S. A.; Wei, P. K.; Fann, W. S. *J. Am. Chem. Soc.* **2001**, *123*, 2296; (d) Zhang, Y.; Hu, Y.; Li, H.; Wang, L.; Jing, X.; Wang, F.; Ma, D. *J. Mater. Chem.* **2003**, *13*, 773; (e) Tzanetos, N. P.; Kallitsis, J. K. *Chem. Mater.* **2004**, *16*, 2648.
5. Tokuhisa, H.; Era, M.; Tsutsui, T.; Saito, S. *Appl. Phys. Lett.* **1995**, *66*, 3433.
6. (a) Karamysheva, L. A.; Torgova, S. I.; Agafonova, I. F.; Petrov, V. F. *Liq. Cryst.* **2000**, *27*, 393; (b) Wild, J. H.; Bartle, K.; Kirkman, N. T.; Kelly, S. M.; O'Neill, M.; Stirner, T.; Tuffin, R. P. *Chem. Mater.* **2005**, *17*, 6354.
7. (a) Hegmann, T.; Neumann, B.; Wolf, R.; Tschierske, C. *J. Mater. Chem.* **2005**, *15*, 1025; (b) Xu, Y.; Li, B.; Liu, H.; Guo, Z.; Tai, Z.; Xu, Z. *Liq. Cryst.* **2002**, *29*, 199; (c) Sato, M.; Mizoi, M.; Uemoto, Y. *Macromol. Chem. Phys.* **2001**, *202*, 3634; (d) Barche, J.; Janietz, S.; Ahles, M.; Schmechel, R.; von Seggern, H. *Chem. Mater.* **2004**, *16*, 4286.
8. Dingemans, T. J.; Samulski, E. T. *Liq. Cryst.* **2000**, *27*, 131.
9. Lai, L. L.; Wang, C. H.; Hsieh, W. P.; Lin, H. C. *Mol. Cryst. Liq. Cryst.* **1996**, *287*, 177.
10. (a) Lai, C. K.; Ke, Y. C.; Su, J. C.; Chen, C. S.; Li, W. R. *Liq. Cryst.* **2002**, *29*, 915; (b) Zhang, Y. D.; Jespersen, K. G.; Kempe, M.; Kornfield, J. A.; Barlow, S.; Kippelen, B.; Marder, S. R. *Langmuir* **2003**, *19*, 6534.
11. (a) Binnemans, K. *Chem. Rev.* **2005**, *105*, 4148; (b) Haristoy, D.; Tsiourvas, D. *Chem. Mater.* **2003**, *15*, 2079; (c) Celso, F. L.; Pibiri, I.; Triolo, A.; Triolo, R.; Pace, A.; Buscemib, S.; Vivona, N. *J. Mater. Chem.* **2007**, *17*, 1201.
12. Kim, B. G.; Kim, S.; Park, S. Y. *Tetrahedron Lett.* **2001**, *42*, 2697.
13. Serrano, J. L. *Metallomesogens; Synthesis, Properties, and Applications*; VCH: New York, NY, 1996.
14. (a) Bu, X. H.; Liu, H.; Du, M.; Zhang, L.; Guo, Y. M.; Shionoya, M.; Ribas, J. *Inorg. Chem.* **2002**, *41*, 1855; (b) Shao, P.; Huang, B.; Chen, L.; Liu, Z.; Qin, J.; Gong, H.; Ding, S.; Wang, Q. *J. Mater. Chem.* **2005**, *15*, 4502; (c) Huang, P. H.; Shen, J. Y.; Pu, S. C.; Wen, Y. S.; Lin, J. T.; Chou, P. T.; Yeh, M. C. P. *J. Mater. Chem.* **2006**, *16*, 850.
15. (a) Incarvito, C.; Rheingold, A. L.; Qin, C. J.; Gavrilova, A. L.; Bosnich, B. *Inorg. Chem.* **2001**, *40*, 1386; (b) Dong, Y. B.; Cheng, J. Y.; Huang, R. Q.; Smith, M. D.; Loye, H. C. *Inorg. Chem.* **2003**, *42*, 5699; (c) Richardson, C.; Steel, P. J.; D'Alessandro, D. M.; Junk, P. C.; Keene, F. R. *J. Chem. Soc., Dalton Trans.* **2002**, 2775; (d) Huang, H.; Song, H. B.; Du, M.; Chen, S. T.; Bu, X. H. *Inorg. Chem.* **2004**, *43*, 931; (e) Dong, Y. B.; Cheng, J. Y.; Wang, H. Y.; Huang, R. Q.; Tang, B. *Chem. Mater.* **2003**, *15*, 2593; (f) Wang, J.; Wang, R.; Yang, J.; Zheng, Z.; Carducci, M. D.; Cayou, T.; Peyghambarian, N.; Jabbour, G. E. *J. Am. Chem. Soc.* **2001**, *123*, 6179.
16. Dong, Y. B.; Ma, J. P.; Huang, R. Q.; Smith, M. D.; Loye, H.-C. Z. *Inorg. Chem.* **2003**, *42*, 294.
17. Wen, C. R.; Wang, Y. J.; Wang, H. C.; Sheu, H. S.; Lee, H. H.; Lai, C. K. *Chem. Mater.* **2005**, *17*, 1646.
18. (a) Kaim, L. E.; Menestrel, I. L.; Morgrntin, R. *Tetrahedron Lett.* **1998**, *39*, 6885; (b) Young, J. R.; DeVita, R. J. *Tetrahedron Lett.* **1998**, *39*, 3931; (c) Verheyde, B.; Dehaen, D. *J. Org. Chem.* **2001**, *66*, 4062.
19. (a) Sua'rez, M.; Lehn, J. M. *J. Am. Chem. Soc.* **1998**, *120*, 9526; (b) Zimmerman, S. C.; Duerr, B. J. *J. Org. Chem.* **1992**, *57*, 8; (c) Marcus, S. H.; Miller, S. I. *J. Am. Chem. Soc.* **1966**, *88*, 3719.
20. Daniel, D. C.; McHale, J. L. *J. Phys. Chem. A* **1997**, *101*, 3070.
21. Rerek, M. E.; Chen, H. C.; Moore, D. J. *J. Phys. Chem. B* **2001**, *105*, 9355.
22. (a) Doroshenko, A. O.; Posokhov, E. A.; Verezubova, A. A.; Ptyagina, L. M. *J. Phys. Org. Chem.* **2000**, *13*, 253; (b) Mordzinski, A.; Grabowska, A.; Kuhnle, W.; Krowszynski, A. *Chem. Phys. Lett.* **1983**, *101*, 291; (c) Kaufmann, J. M.; Litak, P. T.; Boyko, W. J. *J. Heterocycl. Chem.* **1995**, *32*, 1541; (d) Mizoshita, N.; Suzuki, Y.; Hanabusa, K.; Kato, T. *Adv. Mater.* **2005**, *17*, 692; (e) Wash, P. L.; Maverick, E.; Chiefari, J.; Lightner, D. A. *J. Am. Chem. Soc.* **1997**, *119*, 3802.
23. McCubbin, J. A.; Tong, X.; Zhao, Y.; Snieckus, V.; Lemieux, R. P. *Chem. Mater.* **2005**, *17*, 2574.
24. (a) Rieker, J.; Schmitt, E. L.; Birbaum, J. L. *J. Phys. Chem.* **1992**, *96*, 10225; (b) Glemza, A. J.; Mardis, K. L.; Payne, G. F. *Ind. Eng. Chem. Res.* **2000**, *39*, 463; (c) Tobita, S.; Yamamoto, M.; Shizuka, H. *J. Phys. Chem. A* **1998**, *102*, 5206.
25. (a) Jang, W. G.; Park, C. S.; Kim, K. H.; Glaser, M. A.; Clark, N. A. *Phys. Rev. E* **2000**, *62*, 5027; (b) Kasha, M.; Heldt, J.; Gormin, D. *J. Phys. Chem.* **1995**, *99*, 7281; (c) Gormin, D.; Sytnik, A.; Kasha, M. *J. Phys. Chem. A* **1997**, *101*, 672; (d) Ma, D.; Liang, F.; Hung, L. S. *Chem. Phys. Lett.* **2002**, *358*, 24.
26. Schmidtke, S. J.; Underwood, D. F.; Blank, D. A. *J. Phys. Chem. A* **2005**, *109*, 7033.